Photodynamics of charge transfer and ion-pair states of Cl_2:Xe complexes in liquid Ar

M. H. Hill and V. A. Apkarian
Department of Chemistry, University of California, Irvine, California 92717

(Received 12 April 1996; accepted 4 June 1996)

Sequential two photon studies of Xe:Cl_2 complexes in liquid Ar are reported. The first photon prepares the excited state complex Xe:$Cl_2(^3\Pi_u)$, which radiatively relaxes with a lifetime of 10 ± 1 μs (22 ± 2 μs for the uncomplexed $Cl_2(^3\Pi_u)$). A second photon accesses either the molecular ion pair state, Xe:Cl^+Cl^-, or the contact charge transfer transition, $Xe^+Cl_2^-$. The latter dissociates to Xe^+Cl^-+Cl even though the product is formed at threshold. The former undergoes charge rearrangement and decays radiatively via $Xe^+Cl_2^-$ $(^2\Sigma_u)\rightarrow XeCl_2(^1\Sigma_g)$. Analysis of the excitation and emission spectra of the key intermediate in laser induced harpoon reactions, $Xe^+Cl_2^-$, leads to the conclusions that the complex is linear in both ionic and neutral states, and allows a direct contrast between dissociation dynamics on ionic versus neutral surfaces. © *1996 American Institute of Physics.* [S0021-9606(96)02134-4]

I. INTRODUCTION

Laser induced harpoon reactions, the most common of which are those between rare gas atoms (Rg) and molecular halogens (X_2) or halogen containing polyatomic molecules (RX), have been extensively studied in the gas phase,[1–8] in clusters produced in molecular beams,[9–11] in the solid state,[12–16] and in the liquid phase.[13,14,17–19] This class of photochemical reactions is useful in studies of fundamental chemical dynamics, and in particular, bimolecular chemistry, in condensed media. Specializing to the case of molecular halogens, the process can be generically summarized as

$$Rg+X_2+h\nu\rightarrow[Rg+X_2^-]\rightarrow Rg^+X^-+X. \quad (1)$$

The salient features, and the wealth of processes that can be interrogated via this reaction, can be recognized by noting the variety of entrance channels that lead to the key intermediate, the $Rg^+X_2^-$ charge transfer complex.

The most direct analogy with the classic harpoon reaction,[20] the prototype of which is the reaction of an alkali atom with a molecular halogen,[21] is realized by initial excitation of the rare gas atom to a Rydberg state, Rg*.[22,23] Due to its reduced ionization potential, Rg* can be regarded as a pseudoalkali:

$$Rg+(n)h\nu\rightarrow Rg^*, \quad (2a)$$

$$Rg^*+X_2\rightarrow[Rg^+X_2^-]\rightarrow Rg^+X^-+X. \quad (2b)$$

Thus, in an otherwise unreactive solution of X_2/Rg, one- or multiphoton resonant excitation of the rare gas creates the reactive pseudo alkali, and affords the staging of the bimolecular harpoon reaction. An important distinction between the gas and condensed phases in this case is the excitonic nature of the initial state prepared when Rg constitutes the solvent, or the host.[16,18]

Initial excitation of the molecular halogen to an ion-pair state provides an alternate entrance channel to the same dynamics especially in the case of Rg=Xe:

$$X_2+(n)h\nu\rightarrow X^+X^-, \quad (3a)$$

$$X^+X^-+Xe\rightarrow[Xe^+X_2^-]\rightarrow Xe^+X^-+X. \quad (3b)$$

The reactivity of the ion-pair state in Eq. (3b) is guaranteed where the ionization potential of Rg is less than that of the halogen: Rg=Xe, X=F, Cl; and will generally hold in vertically prepared ion-pair states due to their excessive vibrational energy content, as has been rigorously shown for I_2, Br_2, and ICl.[24] The ultrafast experiments on gas phase Xe+I_2, belong to this class.[25]

Another distinct entrance channel to laser induced harpooning is via photoinduced intermolecular charge transfer, i.e., excitation of the contact charge transfer transition, which may be explicitly expressed by the sequence:

$$Rg+X_2\rightleftharpoons[RgX_2], \quad (4a)$$

$$[RgX_2]+(n)h\nu\rightarrow[Rg^+X_2^-]\rightarrow Rg^++X^-+X, \quad (4b)$$

where [RgX_2] is strictly a collision pair. This description is contained in Eq. (1), with the implied emphasis that the process is an n+two-body scattering event, where n is the number of photons involved. Distinguishing this cooperative process from those of Eqs. (2) and (3), is a nontrivial experimental task. The situation is particularly complicated in the case of two-photon excitation due to interference from yet another channel, namely that of photodissociation followed by photoassociation:[26,27]

$$X_2+h\nu\rightarrow X+X, \quad (5a)$$

$$X+Rg+h\nu\rightarrow Rg^+X^-, \quad (5b)$$

in which the photoassociation process of Eq. (5b) again represents excitation of an interatomic transition, a transition of the [RgX] collision complex.

In ultrafast measurements with 100 fs time resolution, and by a proper choice of wavelength, it was possible to single out the process of Eq. (4b) for an unequivocal demonstration of this channel in solutions of Cl_2/LXe.[19] This observation has been more recently verified by time resolved measurements in clusters containing Cl_2 and Xe.[10] In the latter two color experiments, with a probe wavelength of 308 nm, a delayed transient signal due to the sequential process of Eq. (5) could also be seen. The interesting aspect of this observation is the fact that it is transient, otherwise this is the standard method for probing photodissociation of halogen containing molecules in the gas and condensed media, and has even been applied as an analytical tool for detection of Cl atoms.[28]

Finally, it should be noted that in the case of sequential excitation, either due to rapid recombination, as in condensed media, or by choosing a bound upper state, Eq. (5a) may lead to preparation of an electronically excited state of the molecular halogen, X_2^*. The full set of entrance channels listed above can now be repeated with the electronically excited halogen as reagent:

$$X_2+h\nu\rightarrow X_2^*, \tag{6a}$$

$$X_2^*+Rg+h\nu\rightarrow[Rg^+X_2^-]\rightarrow Rg^+X^-+X, \tag{6b}$$

in which Eq. (6b) should be interpreted as the equivalent of Eq. (1), with its variations Eqs. (2) through (5).

The applications of the above listed reactions to condensed phase chemical dynamics is perhaps obvious. The sudden creation of the pseudo-alkali in Eq. (2) enables the time resolved study of bimolecular reactions. The sudden entrance into the charge transfer complex, via Eq. (3) or Eq. (4), enables the study of solvation and dissociation dynamics on ionic surfaces, and time resolved studies of subsequent bimolecular reactions.[19] The sequential excitation scheme in Eq. (5) enables the investigation of photodissociation dynamics on the X_2^* surface, if dissociative, or vibronic dynamics via Eq. (6), if X_2^* is bound or caged.[13,14,17] Obviously, the source of the wealth of laser induced harpoon reactions is also the source of complication. More often than not, the variety of listed entrance channels coexist in the same system, necessitating indirect interpretations. These complications are relaxed in the study of the Xe:Cl_2 complex in liquid Ar, which we report in this paper. With Cl_2/LAr studies as background, two-color spectroscopy with ns lasers allows a clear demonstration of some of the intermediates and mechanisms which have previously been postulated or advanced through indirect modeling. Included among these are: (a) the direct observation of the $Xe^+Cl_2^-$ intermediate in its various electronic states; (b) a direct demonstration of the contrast between reactive dynamics on covalent versus ionic surfaces in condensed media; (c) relative energetics of solvated molecular ion-pair states and intermolecular charge transfer states, and their associated dynamics; (d) observation of the predicted dramatic lowering of intermolecular charge transfer resonances from excited $Cl_2(A/A')$ versus $Cl_2(X)$ states controlled by vertical electron affinities;[17] (e) characterization of the neutral Xe:Cl_2 complex in its various electronic states. The ground state of this complex has been studied in molecular beams,[29] and considered theoretically,[30] as a van der Waals complex which shows incipient bonding. Two-photon induced harpoon reactions of the bare Xe:Cl_2 complex have also been reported.[9,10] A comparison of the liquid phase data with those in the gas phase allows the consideration of effects of solvation on structure and reactivity of this relatively simple model system.

The experimental paradigm and design has been completely discussed previously,[17] we repeat it here succinctly. In solutions of Cl_2/LAr, we first excite Cl_2 to its dissociative $^1\Pi_u$ surface.[31] Due to the strong cage effect, the molecule is reformed populating the bound electronic surfaces—X, A, and A'—that correlate with $Cl(^2P_{3/2})+Cl(^2P_{3/2})$.[32] This is verified by a second laser tuned to promote the A/A' population to the molecular ion-pair states the energetics of which are well established from studies in solid Ar.[33,34] While strongly solvated, the ionic states fluoresce without further chemistry. This serves as the background to interpret experiments in ternary Cl_2/Xe/LAr solutions. Xe:Cl_2 complexes can now be probed directly: excitation of the intermolecular charge transfer state $Xe^+Cl_2^-(^2\Pi_g)$, leads to emission from solvated Xe^+Cl^- and $Xe_2^+Cl^-$ exciplexes;[13] while excitation to the molecular ion-pair state leads to emission from the $Xe^+Cl_2^-(^2\Sigma_u)$. As we argue, the latter emission had previously been observed but misassigned.

II. EXPERIMENT

The experiments were carried out in a three window cryocell attached to an all monel gas handling manifold. The cell is constructed of Be:Cu and electroplated with rhodium. Sapphire windows, sealed with indium gaskets, are used on all three sides. A closed-cycle He cryostat (CTI-22) is used to cool the cell. Temperature is measured with a thermocouple, and regulated to within 0.1 K with a 25 W heater. The cell and manifold were passivated with Cl_2 prior to sample preparation. The Cl_2 (Matheson) was purified by pumping on it in a liquid nitrogen trap. Xe of 99.999% purity (Spectra Gases) and Ar of 99.999% purity (Matheson) were used without further purification. The majority of data was acquired at 100 K in solutions of liquid argon, under its saturated vapor pressure. Experiments were carried out in either binary, Cl_2/LAr, or ternary, Xe/Cl_2/LAr, solutions, at various concentrations of Xe and Cl_2.

Two lasers were utilized with beams counter propagating in the cell. A XeCl laser (Lambda Physik EMG 101) operating at 308 nm, with a 20 ns pulse width and typical energies of 50–100 μJ, was used as the initial excitation source. The second pulse, at 325 or 250 nm with 12 ns pulse width and a typical energy of 30 μJ per pulse, was obtained as the doubled output of an excimer-pumped dye laser (Lambda Physik EMG 201 MSC/FL 3002). Fluorescence was measured at 90° to excitation through a Jarrell Ash monochromator (model 82-410) using a photomultiplier tube (Hamamatsu 666). Data was collected with a digitizing oscilloscope (Tektronix 2430), controlled via a personal computer (AST 286). Spectra were recorded with an optical multichannel analyzer (EG&G OMA3).

III. RESULTS

Emission spectra obtained by sequential excitation of a solution of Xe/Cl_2/LAr are shown in Fig. 1. The spectrum in

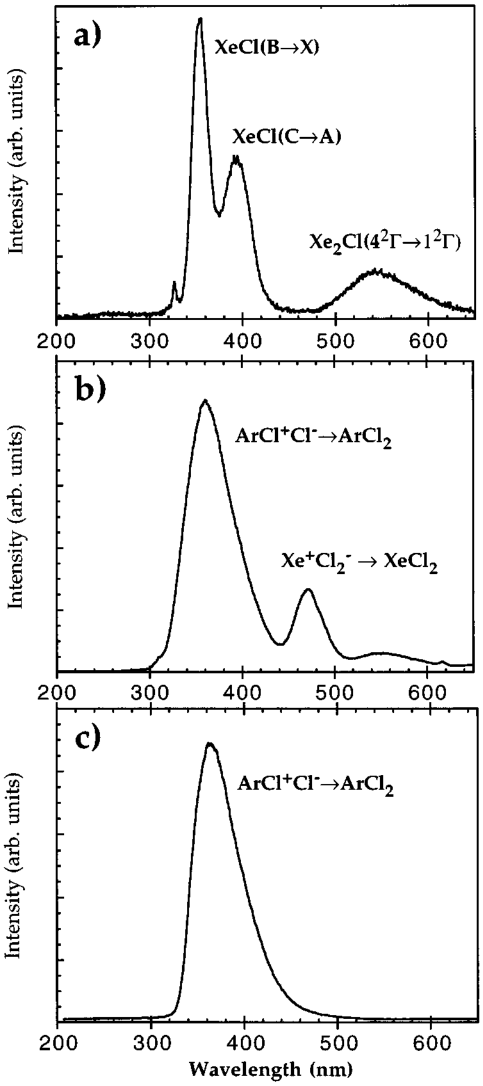

FIG. 1. Fluorescence spectra: (a) ternary solution of Cl$_2$/Xe/LAr excited by 308 nm+325 nm sequence; (b) ternary solution of Cl$_2$/Xe/LAr excited by 308 nm+250 nm sequence; (c) binary solution of Cl$_2$/LAr excited by the 308 nm+250 nm sequence.

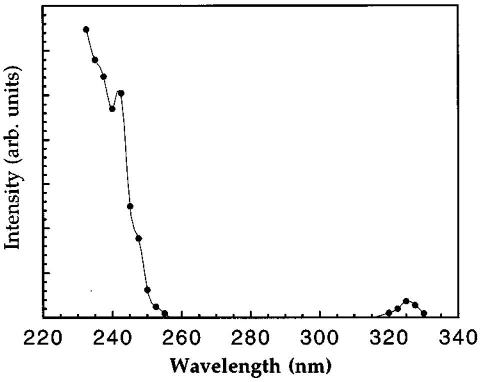

FIG. 2. Discrete excitation spectrum obtained by monitoring fluorescence at 355 nm. The continuous curve is a spline fit to the discrete experimental points.

Fig. 1(a) is obtained by sequential excitation: 308 nm followed by 325 nm excitation. The spectrum consists of the solvated XeCl($B \rightarrow X$) and XeCl($C \rightarrow A$) transitions at 355 nm and 395 nm, respectively; and the broad Xe$_2$Cl emission near 550 nm.[13] The XeCl B and C states are in collisional equilibrium, and relax with an average radiative lifetime of 38±3 ns, while the triatomic exciplex relaxes with its radiative lifetime of 200 ns. These transitions and lifetimes have been well established previously, both in liquid[13] and solid Ar.[12] They are redshifted from their gas phase values by ~0.5 eV, due to solvation of the ionic upper states in the dielectric of the medium. The dielectric of the medium also effects a shortening of radiative lifetimes, such that $\tau_l/\tau_g \sim 0.6$.[35] Taking this effect into account, using the gas phase radiative lifetimes for $B \rightarrow X$ and $C \rightarrow A$ transitions of 13 and 130 ns, respectively, we may conclude from the observed lifetime for these states that the ordering between B and C states is the same as in the gas phase,[36] B is above C by ~70 cm^{-1}.

Excitation of the same solution with the sequence 308 nm+250 nm leads to the spectrum in Fig. 1(b). Three broadbands peaking at 360, 470, and 550 nm, with identical lifetimes of 52±4 ns, are now observed. These broadbands are somewhat distorted, and there is evidence that the spectrum of Fig. 1(c) also contributes to this spectrum.

In binary solutions of Cl$_2$/LAr, the 308 nm+325 nm excitation sequence does not lead to an observable emission, while 308 nm+250 nm excitation leads to the single emission band at 360 nm shown in Fig. 1(c). The measured lifetime of this emission is 48±4 ns. Clearly, the 470 and 550 nm bands observed in Fig. 1(b) are associated with Xe while the 360 nm band observed in Fig. 1(c) is not.

A discrete excitation spectrum, by monitoring fluorescence at 355 nm which is common to all spectra, was obtained with the pump wavelength fixed at 308 nm while scanning the probe wavelength. This is shown in Fig. 2. Two excitation channels can be identified. The strong absorption at wavelengths below 255 nm, leads to the emission observed in Fig. 1(b); while the weaker absorption centered at 325 nm yields the emission spectrum in Fig. 1(a).

The lifetime of the intermediate state involved in the sequential excitation scheme is obtained by monitoring the LIF intensity as a function of delay between pump and probe lasers. In all cases the LIF rise time is laser limited—faster than 10^{-8} s—however, the decay is measurable. The delay dependence for 308 nm+250 nm excitation, while monitoring the 360 nm emission, is shown in Fig. 3. The observed decay is exponential with a lifetime of 22±2 μs. The delay dependence for the 308 nm+325 nm excitation, while monitoring emission at 355 nm, is also shown in Fig. 3. The decay in this case has a lifetime of 10±1 μs. These decay times were established to be independent of both Xe and Cl$_2$ concentrations, for concentrations ranging from 50 to 1000 ppm in each. The independence of decay times on the Cl$_2$ concentration is illustrated in the inset to Fig. 3.

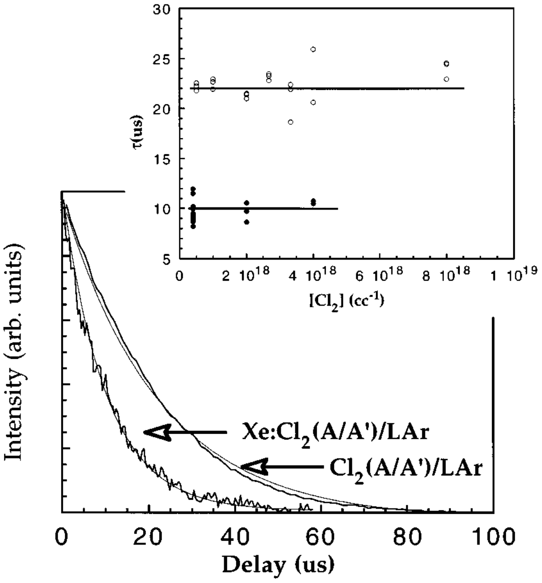

FIG. 3. Lifetime of $Cl_2(A/A')$ measured as a function of delay between pump and probe lasers. The $Cl_2(A/A')$ is prepared in Cl_2/Xe/LAr by dissociative pumping at 308 nm, and probed via laser induced fluorescence from the ion pair state accessed at 250 nm and monitored at 360 nm. The (A/A') state in the Xe:Cl_2 complex is prepared by 308 nm excitation, and probed via laser induced fluorescence from the intermolecular charge transfer state accessed at 325 nm and monitored at 355 nm.

IV. DISCUSSION

A. The intermediate state

Based on the delay dependence of the signals, it is clear that in these sequential two-photon excitations, an intermediate state with a lifetime of $\sim 10^{-5}$ s is being formed. Assignment of this state to $Cl_2(A/A')$ is straightforward. At 308 nm, the absorption in Cl_2 is to the repulsive $^1\Pi_u$ state. However, this excitation does not lead to permanent dissociation of the molecule in liquid Ar. Had such a channel existed, we would expect, at the experimental concentrations, a diffusion controlled risetime of $\sim 10^{-7}$ s for the formation of XeCl(X), which would serve as the intermediate state in accessing Xe^+Cl^- with UV excitation [as in Eq. (5)]. This, for example, is the case for F_2 dissociation in F_2/Xe/LAr solutions.[37] Evidently, as in the case of solid Ar,[13,32] at this excitation energy, the cage effect is complete for Cl_2 in liquid Ar. Geminate recombination, in addition to formation of $Cl_2(X)$, leads to population trapping in the A/A' states. The latter are the only bound electronically excited states that correlate with $Cl(^2P_{3/2})+Cl(^2P_{3/2})$.

The observed variation of the $Cl_2(A/A')$ relaxation time in the different solutions is noteworthy. We expect the nested $A(^3\Pi_{1u})$ and $A'(^3\Pi_{2u})$ states to be in collisional equilibrium in the 100 K liquid. The strongly forbidden $A' \rightarrow X$ emission in solid Ar has a radiative lifetime of 73 ms,[32] while the $A \rightarrow X$ emission can be expected to be several orders of magnitude shorter.[38] The observed lifetimes of $\sim 10^{-5}$ s, which do not show dependence on Xe or Cl_2 concentration, are then dominated by $A \rightarrow X$ radiation (which must be enhanced in the liquid phase by intensity borrowing from $B \rightarrow X$). The situation is quite similar to that of Br_2 in Liquid Xe, which has previously been studied by the same method as in the present.[17] It is also well established that the radiative lifetimes of these forbidden transitions are shortened in the series Ar, Kr, Xe.[38] The observation of a 22 μs lifetime for the A/A' states while monitoring the 360 nm emission, which does not involve Xe, and a lifetime of 10 μs while monitoring the XeCl emissions, is consistent with the expectation that Xe enhances the radiative coupling of A to X. The rationale, however, leads to the conclusion that Xe remains complexed to $Cl_2(A/A')$, and does not exchange with Ar for the duration of the excited state lifetime. This in turn would imply that there is a significant barrier to the exchange reaction, or equivalently, to the unimolecular dissociation of the complex. Even if the solvent structure were taken into account, the stability of this excited state complex cannot be rationalized based on van der Waals binding alone. Had that been the case, then the complex would dissociate on the time scale of the elementary step of diffusion, $\sim 10^{-11}$ s. The observed lower limit for this process of 10^{-5} s implies a lower limit of ~ 0.25 eV for the free energy barrier to exchange between Xe and solvent Ar.

We are forced to conclude incipient chemical bonding between Xe and $Cl_2(A/A')$, as suggested previously for the ground state complex Xe:$Cl_2(X)$.[29,30] Further stabilization of the complex in the excited $Cl_2(A/A')$ state, which has an electron configuration $\sigma_g^2\pi_u^4\pi_g^3\sigma_u^1$, must be attributed to partial charge transfer from the polarizable Xe to the hole in the π_g molecular orbital. This can be regarded as a mixing between covalent and ionic states, an effect that will be enhanced upon solvation due to lowering of the ionic potentials. In the absence of a quantitative analysis, this consideration alone does not suggest an obvious structure for the complex. However, given the stability of the complex, we may limit our consideration to the linear and T-shaped possibilities.

B. Excitation resonances

The two resonances observed in the excitation spectrum of Fig. 2 can be interpreted based on energetics alone. The 250 nm excitation, which is present in the binary Cl_2/LAr solutions, can uniquely be assigned to access of the lower tier of $Cl^+(^3P_2)Cl^-(^1S)$ ion-pair states, via the $D' \leftarrow A'$ transition.[39] Using the known potential parameters for the free molecule, the observed vertical transition at 250 nm implies electronic solvation of the $Cl^+Cl^-(D')$ state by 0.5 eV (see Fig. 4). This is consistent with what is observed for the equivalent transitions of I_2 in solid Ar,[40] and characteristic of solvation of a dipole of a full charge separation at a distance of ~ 3 Å, as in the cases of Xe^+Cl^- and $Xe_2^+Cl^-$ already encountered above.

The 325 nm excitation occurs significantly below the first molecular ionic transition, yet it leads to formation of xenon chloride exciplexes, it must therefore, be assigned to the contact charge transfer transition: $Xe^+Cl_2^- \leftarrow XeCl_2(^3\Pi_u)$. We will consider the energetics of this transition, and the charge configurations that are implied, in terms of diatomic

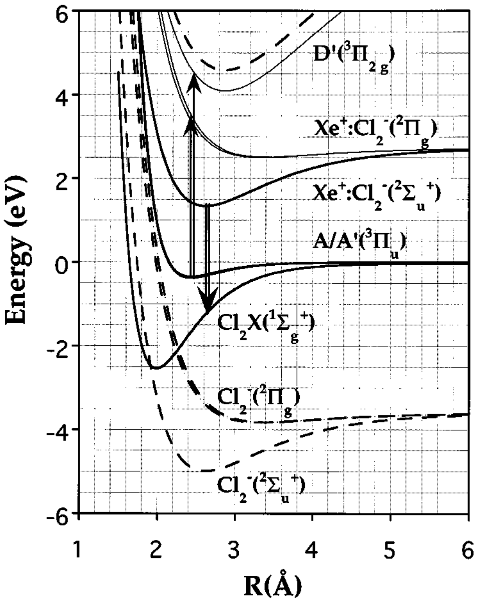

FIG. 4. A partial energy level diagram of the relevant solvated electronic states along the Cl–Cl coordinate. The dashed curves are for the unperturbed gas phase potentials. The ion-pair state is electronically solvated by 0.5 eV, as verified from the $Cl_2(D' \leftarrow A')$ resonance at 255 nm, which is indicated by the up-arrow. The excitation resonance for the intermolecular charge transfer transition, $Xe{:}Cl_2(^2\Pi_g) \leftarrow Xe{:}Cl_2(A')$ at 325 nm is indicated by the shorter up-arrow. The upper state is located according to Eq. (7) of the text. The fluorescence of the charge transfer complex, $Xe^+Cl_2^-(^2\Sigma_u) \rightarrow XeCl_2(^1\Sigma_g)$ which occurs at 470 nm, is indicated by the double arrow pointing down. The figure also enables the identification of the vertical electron affinities of Cl_2 which depend on the choice of initial and final states.

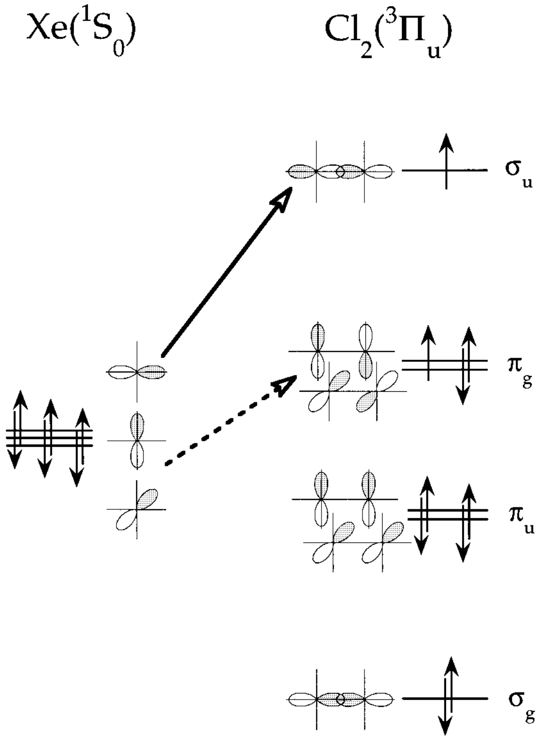

FIG. 5. The possible intermolecular charge transfer transitions in the $XeCl_2(^3\Pi_u)$ complex are indicated. The solid arrow corresponds to the observed excitation transition, while the allowed dashed arrow corresponds to the unobservable transition.

fragments in the triatomic complex, in the spirit of diatomics-in-ionic-systems.[41] Consideration of the molecular orbital diagram of Cl_2 in Fig. 5, makes it clear that two contact charge transfer transitions are possible: electron transfer from Xe, to either the π_g or the σ_u molecular orbital, to prepare either $Cl_2^-(^2\Sigma_u)$ or $Cl_2^-(^2\Pi_g)$, respectively.[42] With the aid of Fig. 4, it can be verified that in a vertical electron transfer, the first transition creates the Cl_2^- fragment near the minimum of its bound ground state; while the second transition prepares the molecular ion on its dissociative curve. Only the latter is consistent with the experiment. This can be established with the data contained in the experiment. Thus, taking the binding energy of $Cl_2(A')$ of 0.31 eV into account, 325 nm promotes the system to 3.5 eV above the Xe+Cl+Cl asymptote. The vibrationally equilibrated product $Xe^+Cl^-(B)$ emits a 3.5 eV photon (355 nm) in its radiative dissociation to the same Xe+Cl+Cl asymptote. The photon therefore does not contain the additional 1.48 eV which would be required to overcome the binding of $Cl_2^-(^2\Sigma_u)$. The Xe^+Cl^- is therefore prepared cold, near thermodynamic threshold, on a surface consistent only with $Cl_2^-(^2\Pi_g)$ in which the Cl–Cl coordinate is unbound.

The consistency of the above conclusion can be further tested. The vertical charge transfer transition energy of the complex, can be estimated as[43]

$$h\nu = \mathrm{IP}[\mathrm{Xe}] - \mathrm{EA}^v[Cl_2(A/A')] - e^2/r_c - \Delta E_s, \tag{7}$$

in which IP[Xe} is the ionization potential of Xe=12.13 eV, EA^v is the vertical electron affinity of the electronically excited Cl_2 which depends on the choice of states, the third term is the Coulombic stabilization of the charge transfer state at the contact distance r_c between Xe and Cl_2, and $\Delta E_s \sim 0.5$ eV, represents the differential solvation of the ionic and neutral states in liquid Ar. Thus the first three terms in Eq. (7) are appropriate for the gas phase intermolecular charge transfer at contact, and the effect of the dielectric is entirely accounted by the last term. Using the Cl_2^- potentials of Chen and Wentworth,[42] the vertical electron affinities as measured from the minimum of $Cl_2(A')$ are 2.7 and 4.5 eV, for transitions terminating on $Cl_2^-(^2\Pi_g)$ and $Cl_2^-(^2\Sigma_u)$, respectively. If we assume $r_c = 3.2$ Å, i.e., that of the Xe–Cl pair minimum,[44] then 325 nm implies a vertical electron affinity of 3.3 eV. This value cannot be reconciled with a transition terminating on $Cl_2^-(^2\Sigma_u)$, but would be consistent with a transition to $Cl_2^-(^2\Pi_g)$ if the Cl–Cl bond length in the complex were stretched out to 2.9 Å. Thus, with a reasonable modification of bond lengths away from their separated pair values in the $Xe{:}Cl_2(A/A')$ complex, e.g., a Cl–Cl bond length of 2.8 Å and a Xe–Cl bond length of 3.1 Å, the observed transition can be unambiguously established as terminating on $Cl_2^-(^2\Pi_g)$. The extracted structure will certainly have significant uncertainty due to the estimate of solvation and uncertainty in the negative ion potentials. What is certain, however, is the assignment of the transition, and the trend that the Cl_2 bond length is somewhat longer in the complex, and that the Xe is more tightly bound than what would be expected based on van der Waals parameters. The latter conclusion was also reached on the basis of the lifetime of the complex.

In summary, based on energetic grounds alone, we can conclude that the vertical excitation at 325 nm prepares the charge transfer state of the complex on a surface that directly correlates with the two fragment electronic states: $Xe^+(^2P)+Cl_2^-(^2\Pi_g)$ and $Xe^+Cl^-(^2\Sigma_{1/2})+Cl(^2P_{3/2})$.

C. Assignment of emission spectra

The photodynamics subsequent to 308 nm+250 nm excitation in the binary solutions of Cl_2/LAr are nearly identical to what is observed in solid Ar.[33,34] The 250 nm photon prepares the Cl^+Cl^- ion-pair state, which is shifted by ~0.5 eV relative to its gas phase energy due to electronic solvation in the dielectric of the medium. The known[45] strong binding in $ArCl^+$ leads to complexation of the ion-pair state with the solvent, which is reflected by the dramatic Stokes shift of ~1.5 eV observed between excitation (250 nm) and emission (360 nm). Note, that in this case, the larger ionization potential of Ar implies that the $Ar^+Cl_2^-$ states are significantly above those of $ArCl^+Cl^-$.

The photodynamics due to the 308 nm+250 nm excitation sequence of the Xe:Cl_2 complexes in liquid Ar, differs from the case of Cl_2/LAr, by the fact that the intermolecular charge transfer states are now lower in energy than the molecular ion-pair state. It was experimentally established that the 470 and 550 nm emissions are due to charge transfer states containing Xe, and given the fact that they relax with the same rate, they are likely to originate from the same upper state. In the absence of lifetime measurements, spectroscopically, it would be difficult to distinguish the 550 nm emission from that of the $Xe_2^+Cl^-$ emission, and could have been overlooked in prior studies. However, the 470 nm band had previously been observed by multiphoton excitation of ternary solutions at 308 nm, and had been assigned to the mixed triatomic exciplex $(XeAr)^+Cl^-$.[13] The absence of the 470 nm band in the spectrum of Fig. 1(a), which contains the spectra of Xe^+Cl^- in liquid Ar, makes that assignment unacceptable. The 250 nm excitation in this case prepares the ion-pair state of Cl_2 with a Xe as nearest neighbor, Xe:Cl^+Cl^-. Charge rearrangement in this case should lead to the lowest of ionic surfaces, to $Xe^+Cl_2^-(^2\Sigma_u^+)$, which would then relax radiatively, via the back charge transfer $Xe^+Cl_2^- \rightarrow XeCl_2$. The observed transition energy can be rationalized using Eq. (7), but now using the adiabatic electron affinity of Cl_2 since the emission is from the relaxed state. Assuming $r_c=3$ Å, consistent with the determination from the excitation resonance, the ionic state can be located at 1.83 eV above the Xe+Cl+Cl asymptote. The observed emission at 2.64 eV (470 nm) implies that the emission must terminate 0.8 eV below the dissociation limit of Cl_2. This establishes the terminal state of the transition as $Cl_2(X)$, and yields an estimate for the Cl–Cl bond length in the ionic complex of 2.9 Å. A more careful estimate, including Xe–Cl repulsive energy on the neutral surface, places this closer to 2.95 Å. The more robust conclusion is the fragment correlations associated with the 470 nm transition: namely $Cl_2^-(^2\Sigma_u^+) \rightarrow Cl_2(^1\Sigma_g^+)$ and $Xe^+Cl^- \rightarrow XeCl(X)$. The broad emission at 550 nm from the same upper state can therefore be ascribed to termination on the XeCl(A) surface. Indeed, both the separation between these emissions and their widths parallel those of XeCl $B \rightarrow X$ and $C \rightarrow A$ transitions.

The above revision of the 470 nm emission, also applies in its entirety to an assignment made in ternary solids of Cl_2/Xe/Ne, in which in addition to observing all of the xenon chloride exciplexes, a band at 430 nm (2.89 eV) was assigned to $(XeNe)^+Cl^-$.[46] That inconsistency, namely the coexistence of Xe^+Cl^- and a distinct $(XeNe)^+Cl^-$ in a Ne host can be eliminated in kind, by reassigning the emission to $Xe^+Cl_2^-$ in Ne. The difference in emission peaks of 0.24 eV between Ne and Ar, agrees with the expected difference solvation of the ionic state. The issue of which mixed triatomic exciplexes, $(RgRg')^+X^-$, can be formed in a given rare gas host has been considered previously.[47] The only definite assignments are for those where Rg and Rg′ are from neighboring rows. The only outliers to this rule $(XeAr)^+Cl^-$ and $(XeNe)^+Cl^-$ are reassigned here. A simple generalization can be made. Only for systems where the binding energy of $(RgRg')^+$ is larger than the dipole induced dipole interaction of Rg^+X^- and Rg′ will there be a definite mixed triatomic complex formed. This conclusion holds for all the known mixed triatomic exciplexes, as can be verified by the data collected in Table III of Ref. 47.

D. Structure of the cluster

The observed excitation resonance in the complex was established above to correlate with the $Cl_2^-(^2\Pi_g) \leftarrow Cl_2(^3\Pi_u)$ transition and not with $Cl_2^-(^2\Sigma_u) \leftarrow Cl_2(^3\Pi_u)$. These transitions are illustrated respectively by the solid and dashed arrows in Fig. 5. The observed emission correlates with $Cl_2^-(^2\Sigma_u) \rightarrow Cl_2(^1\Sigma_g)$, the reverse of the solid arrow in Fig. 5, but now π_g is doubly occupied. The observed transitions show an apparent $u \leftrightarrow g$ and $\Delta\Lambda=0$ propensity, dictated by the Cl_2 moiety. These are not strict selection rules. For any symmetry of the triatomic Xe–Cl_2 complex, be it linear, C_{2v}, or C_s, there cannot be found strict symmetry arguments to preserve such a selection on the diatomic fragment. The effective observed transitions must therefore, be controlled by the overlap between electron and hole wave functions involved in the optical charge transfer transitions. As we argue below, this consideration leads to the conclusion that the observed transitions are strictly those of the linear complex.

Continuing with our analysis of the complex from its diatomic fragments, we extend in this section the considerations that are well established for the Rg–X fragment. The Xe–Cl pair potentials have been well analyzed theoretically.[48] The interaction energy is minimized for the Σ approach, where the hole on the halogen atom points at the rare gas. This minimizes electron–electron repulsion, and therefore the distance of closest approach. Binding then results from the sum of dispersion forces and ionic admixture

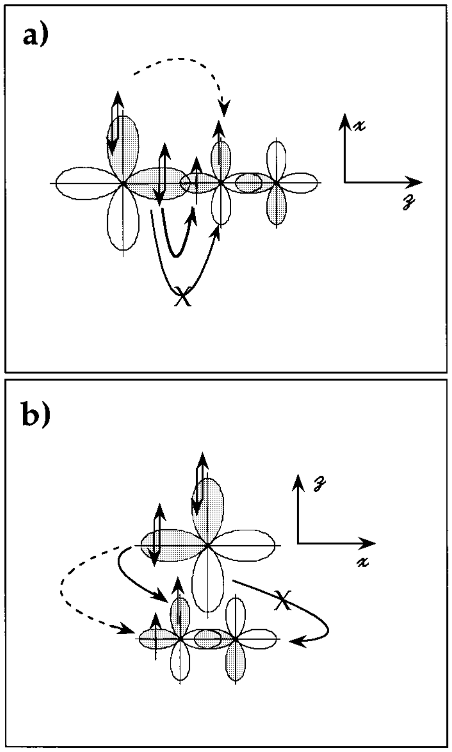

FIG. 6. The relevant atomic orbitals for the intermolecular charge transfer transitions in the XeCl$_2$($^3\Pi_u$) complex are shown for (a) the linear geometry, (b) C_{2v} symmetry. The dashed arrows represent allowed transitions with poor electron-hole overlap. The nonallowed transitions, due to zero overlap, are marked with an *X*.

in the ground state. The intensity of RgX–Rg$^+$X$^-$ transitions is controlled by overlap between electron and hole wave functions, whereby, Σ–Σ and Π–Π transitions are two orders of magnitude larger than Σ–Π transitions.[48] Now consider the complex with the aid of Fig. 6 in which the relevant orbitals, the half filled $\sigma_u(p_z-p_z)$ and $\pi_g(p_x-p_x)$ orbitals of the Cl$_2$ fragment are shown. In either linear or T geometry, the distance of nearest approach is determined by the repulsion between the filled p_z orbital on Xe and the molecular orbitals on Cl$_2$($^3\Pi_u$). This prevents the Xe($p_{x,y}$) orbitals from developing significant overlap with the molecular orbitals, and a transition such as Xe(p_x)→Cl$_2$(π_g) shown with the dashed arrow in Fig. 6(a) will be weaker than the Xe(p_z)→Cl$_2$(σ_u). The latter electron transfer leads to the observed correlation, it leads to Cl$_2^-$($^2\Pi_g$)←Cl$_2$($^3\Pi_u$). Moreover, in this geometry, the Xe$^+$(^2P)Cl$_2^-$($^2\Sigma_u$) ←Xe(^1S)Cl$_2$($^3\Pi_u$) transition which is not observed in excitation, cannot be affected by transfer of the Xe(p_z) electron to the molecular π_g orbital (see Fig. 6). In the T geometry, only the Xe(p_x) has the proper symmetry to transfer an electron to either π_g or σ_u molecular orbitals on Cl$_2$. Overlap considerations [see Fig. 6(b)] make it clear that in this geometry the transfer to π_g, and therefore excitation of Cl$_2^-$($^2\Sigma_u$), would dominate. Thus, the observed and absent excitations are possible to rationalize in the linear geometry, but not in C_{2v}. The neutral complex Xe($^1S_0$):Cl$_2$($^3\Pi_u$) must be linear. Similar considerations apply for the observed emission, which must arise from the ground state of the ionic complex, i.e., from Xe$^+$Cl$_2^-$($^2\Sigma_u$). In the linear geometry, emission can be accomplished via: Xe$^+$(^{2}P[p_x^2,p_y^2,p_z^1])Cl$_2^-$($^2\Sigma_u\,[\sigma_g^2\pi_u^4\pi_g^4\sigma_u^1]$) $\rightarrow$ Xe(^1S)Cl$_2$($^2\Pi_u\,[\sigma_g^2\pi_u^4\pi_g^4\sigma_u^0]$), while in C_{2v} the allowed Cl$_2$(σ_u)→Xe(p_x) transition would have negligible overlap. Note, that based on the radiative lifetime of the upper state, 5×10^{-8} s, the observed transition is strongly allowed. Therefore the observed emission is consistent with the linear geometry and not consistent with the T geometry: Xe$^+$Cl$_2^-$ must also be linear.

We conclude, that the linear geometry, both in the neutral and ionic states of the complex, is consistent with the observed radiative transitions. This does not preclude the existence of dark T-shaped structures in the covalent state. In fact the T-shaped complex of Xe:Cl$_2$ has been observed in molecular beam experiments.[29] Ironically, those experiments cannot exclude the presence of the linear cluster.

E. Solvent assisted dissociation on the ionic surface

The photodynamics in the ternary solutions initiated by the 308 nm+325 nm excitation sequence is rather intriguing. After preparation of Xe:Cl$_2$(A/A') with the 308 nm photon, 325 nm excitation induces the intermolecular charge transfer in the complex. The only emissions observed in this case are those of Xe$^+$Cl$^-$ and Xe$_2^+$Cl$^-$. Evidently, Xe$^+$Cl$_2^-$($^2\Pi_g$) prepared in liquid Ar, dissociates, and the neutral Cl atom is prevented from back reaction with Xe$^+$Cl$^-$. Otherwise, cage induced recombination on the bound Xe$^+$Cl$_2^-$($^2\Sigma_u^+$) surface would occur, and would be observed through its bright emission at 470 nm. The absence of this emission implies permanent dissociation on the ionic surface.

This facile dissociation on the ionic surface is consistent with the linear geometry of the complex. For the charge transfer excitation in the linear geometry it is meaningful to consider creation of an electron localized on the Cl atom closest to Xe$^+$—a closed shell Cl$^-$ ion flanked by the open shell Xe$^+$ and Cl. In such an arrangement the Cl$^-$ would be Coulombically bound to Xe$^+$ and its nonbonded interaction with Cl the other atom would be comparable to that between Cl$^-$ and Ar. Upon the first stretch of the Cl–Cl$^-$ coordinate on its repulsive $^2\Pi_g$ surface, the Xe$^+$Cl$^-$+Cl product would be formed prior to any energy loss. The latter consideration is crucial, since the excitation prepares the system near the threshold of this exit channel. In contrast, in the C_{2v} geometry, the charge would initially be delocalized symmetrically on both Cl atoms. Only after stretching, and interacting with the solvent, would the charge localize. However, in this case, energy loss prior to charge localization would be unavoidable, and a unit dissociation probability would not be possible.

The present experiment most directly illustrates the dramatic contrast between dynamics on ionic and neutral surfaces in condensed media: dissociation is complete on the ionic surface with nearly zero excess energy in the initial preparation, caging is complete on the neutral Cl$_2$ surfaces when prepared with an excess energy of ~1.4 eV. This contrast persists in solids and liquids, has been recognized previously, and has been discussed as the ''negative'' cage effect.[12,13,15] The energy gained by localization of charge on one of the Cl atoms, and the solvation energy by collapse of the cage on the nascent Xe^+Cl^- dipole are the necessary driving forces of dissociation. In effect, a solvent atom inserts between the Xe^+Cl^- and Cl to complete the solvation of the nascent dipole. The product formation is not controlled by repulsive energy release, as would occur in the case of the unsuccessful impulsive dissociation on the covalent $Cl_2(^1\Pi_u)$ dissociative surface; but rather, during the attractive energy release of solvation. The suggested picture is one in which neutral Cl is ejected during the contraction of the Xe^+Cl^- bond with a concerted collapse of the solvent shell on the dipolar moiety.

F. Implications regarding the gas phase complex

The photoinduced harpoon reaction has been studied in Xe:Cl_2 complexes prepared in molecular beams by both one-[10] and two-photon excitation.[9(a),9(b)] These experiments have yielded results that were difficult to comprehend within the model assumptions. No evidence for $Xe^+Cl_2^-$ was found, and the harpooning was completed producing the vibrationally cold Xe^+Cl^- product despite the fact that it was estimated that the product would be formed with an excess energy of 15000 cm^{-1}.[9] Moreover, this result was in sharp contrast with the full collision Xe^*+Cl_2 reaction product of Setser *et al.* where the nascent vibrational population was near $v=100$.[7(b)] A more intriguing observation was also made in the two-photon action spectra. When monitoring the XeCl(B) fluorescence, a structured excitation reminiscent of the XeCl fragment could be observed, while when monitoring the XeCl(C) emission, an unstructured profile was observed.[9(b)] In the more recent one-photon experiments, it was clear that XeCl(B) is formed directly, and that XeCl(C) is formed subsequently through collisions. These results are surprising if two assumptions are made, that the complex is T shaped and that the excitation prepares Xe^+:$Cl_2^-(^2\Sigma_u)$. Our analysis indicates that neither of these assumptions are necessarily valid.

Taking the anisotropy of the Xe–Cl potential into account, it is easy to show that the linear and T complexes of Xe:$Cl_2(X)$ have comparable well depths.[49] In the linear geometry, one-photon induced charge transfer out of the Xe(p_z) orbital would lead to $Xe^+Cl^-(\Sigma)$ which correlates with XeCl(B), consistent with experiment.[10] In the C_{2v} geometry, electron transfer from either Xe(p_x) or Xe(p_z) to either σ_u or π_g molecular orbitals on Cl_2 would lead to a linear combination of Xe^+Cl^- Π and Σ states, and therefore both XeCl B and C would be created directly, in contrast with experiment.[10] While the role of orbital orientations on product selectivity was considered in Ref. 10, it was not recognized that the experiment could not be reconciled with the T geometry, which was assumed to be the more likely possibility. The two-photon coherent excitation of the complex is a two-electron transition, the Xe electron is transferred to Cl_2, and the Cl_2 electron is promoted to the $(^{1,3}\Pi)$ state, and as such yields itself to the analysis presented above for the sequential excitation. Note, in a coherent two-photon excitation both time orderings must be included. In the linear geometry, Cl_2 is promoted to its Π state, and prior to any motion, the Xe electron is transferred to the molecular σ_u orbital. The repulsive energy along the $Cl_2^-(^2\Pi_g)$ surface, is now entirely converted to relative translation of Xe^+Cl^- and Cl. The internal excitation Xe^+Cl^- is entirely controlled by the Franck–Condon accessible region, it will be cold due to the similarity of the Xe–Cl distances in the covalent and ionic states. We may expect the two-photon Franck–Condon spectrum for this complex to be given by the convolution of two one-dimensional spectra, the structured spectrum along Xe–Cl and the continuous spectrum along Cl–Cl, as is observed experimentally when monitoring the XeCl(B). A possible explanation for the difference between this action spectrum and that obtained when monitoring XeCl(C) can be provided, if we assume, that the latter is from C_{2v} complexes. Noting that even after taking spin–orbit interactions into account, the $Xe^+Cl^-(C_{3/2})$ state is nearly purely of $^2\Pi$ character,[48] we recognize that this fragment would correlate with the Xe$(p_x)\rightarrow Cl_2(\pi_g)$ transition which occurs in the T geometry, as indicated in Fig. 6(b). Now the Cl_2^- fragment is borne on its ground surface, and its vibronic states will contribute to the observed two-photon spectrum. The anticipated spectral congestion could explain the absence of structure in this channel.

Given the details of surfaces that are known for this system, it would seem that the above speculations are unnecessary. Detailed theoretical analysis of the spectra and dynamics in various media should be possible, and would be highly illuminating.

V. CONCLUSIONS

In liquid Ar, as in solid Ar, excitation of the $Cl_2(^1\Pi_u \leftarrow {}^1\Sigma_g^+)$ dissociative transition ~1.5 eV above the molecular dissociation limit, leads to no permanent dissociation. The cage effect is complete, the Cl atoms geminately recombine on a time scale shorter than the experimental detection limit of 10^{-8} s. Population trapping in the $A/A'(^3\Pi_u)$ states occurs during recombination.

In binary Cl_2/LAr solutions, the $Cl_2(A/A')$ state is probed via laser induced fluorescence from the molecular ion-pair states. The energetics of the molecular ion-pair states in liquid Ar are nearly identical to those in solid Ar.[33,34] The molecular $D'(^3\Pi_{2g})\leftarrow A'(^3\Pi_{2u})$ transition occurs at 5 eV, red shifted by 0.5 eV from the gas phase due to electronic solvation of the ion-pair state. The emission over the same transition is further shifted to 3.44 eV due to solvent rearrangement and charge localization. Given the strong Ar–Cl^+ interaction, the ion-pair state binds to the solvent atoms, and the emission terminates on the repulsive Ar–Cl wall on the neutral surface. The effective radiative lifetime of the A/A' state in LAr is 22±2 μs.

In ternary Cl_2/Xe/LAr solutions, new excitation and emission bands associated with the Cl_2:Xe complex are observed and analyzed. In addition to the molecular ion-pair states, the $Xe^+Cl_2^-$ intermolecular charge transfer states are now optically accessible from Xe:$Cl_2(A')$. The lifetime of the A/A' state in the complex is 10±1 μs. This also constitutes the lower limit of the lifetime of Xe:$Cl_2(^3\Pi_u)$. The strong binding in this excited state complex is ascribed to partial charge transfer from Xe to the hole in the molecular π_g orbital, an effect that can be expected to be enhanced over the gas phase due to lowering of the ionic excited states. Based on analysis of the contact charge transfer transitions, it is concluded that the Xe–$Cl_2(^3\Pi_u)$ complex is linear in liquid Ar.

The main contact charge transfer absorption of the excited state complex occurs at 325 nm, and leads to formation of Xe^+Cl^- and Cl. The dissociative nature of this transition, and analysis of the energetics of the diatomic fragments within the complex, leads to its assignment as $Xe^+Cl_2^-(^2\Pi_g)\leftarrow Xe{:}Cl_2(^3\Pi_u)$. This assignment is key to the conclusion that the neutral cluster is linear. Excitation of the molecular ion-pair resonance within the complex leads to an emission at 470 nm, which had previously been assigned to $(ArXe)^+Cl^-$, and is presently reassigned to $Xe^+Cl_2^-(^2\Sigma_u^+)\rightarrow XeCl_2(^1\Sigma_g^+)$. The simplest argument for rejecting the previous assignment is that it is possible to prepare the Xe^+Cl^- states in LAr without observing this emission. The same considerations allow reassignment of a 430 nm emission band observed in solid Ne,[46] from $(XeNe)^+Cl^-$ to $Xe^+Cl_2^-$ isolated in Ne. These reassignments bring consistency to the list of mixed triatomic exciplexes observed in condensed phase.[47] They are limited to RgRg$'$ pairs where Rg and Rg$'$ are from neighboring rows. Consideration of the atomic orbitals implicated in this emission leads to the conclusion that $Xe^+Cl_2^-$, which plays the key role in laser induced harpoon reactions, is linear in its ground state.

The dramatic difference between photodissociation on ionic and covalent surfaces, which has been previously noted under the concept of a ''negative'' cage effect,[12,13,15] is clearly demonstrated in these studies. At an excess energy of 1.5 eV, Cl_2 does not undergo permanent dissociation in liquid Ar; while with nearly zero excess energy, $Xe^+Cl_2^-(^2\Pi_g)$ completes the harpoon reaction to dissociate with near unit probability to Xe^+Cl^-+Cl. The formation of this product at threshold is also observed in the two-photon induced harpoon reaction in Xe:Cl_2 complexes prepared in molecular beams.[10] The line of arguments followed in the present study are thought to provide a rationale for some of the surprises found in those studies.

ACKNOWLEDGMENTS

This research was supported through grants from the National Science Foundation, ECS-8914321, and from the US Air Force Office of Scientific Research, AFOSRF49620-1-0251.

[1] S. I. Yakovlenko, Sov. J. Quantum Electron. **8**, 151 (1978).

[2] V. A. Dubov, L. I. Gudzenko, L. V. Gurvich, and S. I. Yakovlenko, Chem. Phys. Lett. **45**, 330 (1977); **46**, 25 (1977); V. S. Dubov, Ya. E. Lapsker, A. N. Samoilova, and L. V. Gurvich, Chem. Phys. Lett. **83**, 518 (1981).

[3] H. P. Grieneissen, Hu Xue-Jing, and K. L. Kompa, Chem. Phys. Lett. **82**, 421 (1981).

[4] B. E. Wilcomb and R. Burnham, J. Chem. Phys. **74**, 6784 (1981).

[5] Y. C. Yu, D. W. Setser, and H. Horiguchi, J. Phys. Chem. **87**, 2209 (1983).

[6] T. O. Nelson, D. W. Setser, and J. Qin, J. Phys. Chem. **97**, 2585 (1993); F. Huang, D. W. Setser, and B. S. Cheong, Isr. J. Chem. **34**, 127 (1994).

[7] J. Qin and D. W. Setser, Chem. Phys. Lett. **184**, 121 (1991); J. Qin, T. O. Nelson, and D. W. Setser, J. Phys. Chem. **95**, 5374 (1991); T. O. Nelson and D. W. Setser, Chem. Phys. Lett. **170**, 430, (1990); J. K. Ku, G. Inoue, and D. W. Setser, J. Phys. Chem. **87**, 2989 (1983).

[8] V. S. Dubov, J. Chem. Phys. **97**, 7342 (1992); K. Babaev and V. S. Dubov, Chem. Phys. Lett. **199**, 93 (1992).

[9] (a) M. Boivineau, J. Le Calve, M. C. Castex, and C. Jouvet, Chem. Phys. Lett. **128**, 528 (1986); (b) C. Jouvet, M. Boivineau, M. C. Duval, and B. Soep, J. Phys. Chem. **91**, 5416 (1987); (c) M. Boivineau, J. Le Calve, M. C. Castex, and C. Jouvet, J. Chem. Phys. **84**, 4712 (1986).

[10] C. Dedonder-Lardeux, M. Berdah, C. Jouvet, S. Martenchar-Barra, J. M. Mestdagh, D. Solgadi, and J. P. Visticot, J. Chem. Phys. **104**, 2740 (1996).

[11] C. Dedonder-Lardeux, C. Jouvet, S. Martenchar-Barra, F. Talbot, and D. Solgadi, Chem. Phys. Lett. **250**, 293 (1996).

[12] M. E. Fajardo and V. A. Apkarian, J. Chem. Phys. **85**, 5660 (1987); **89**, 4102 (1988).

[13] M. E. Fajardo, R. Withnall, J. Feld, F. Okada, W. Lawrence, L. Wiedeman, and V. A. Apkarian, Laser Chem. **9**, 1 (1988).

[14] F. Okada, L. Wiedeman, and V. A. Apkarian, J. Phys. Chem. **93**, 1267 (1989).

[15] H. Kunttu, J. Feld, R. Alimi, and V. A. Apkarian, J. Chem. Phys. **92**, 3551 (1990); A. I. Katz and V. A. Apkarian, J. Phys. Chem. **94**, 6671 (1990).

[16] W. G. Lawrence and V. A. Apkarian, J. Chem. Phys. **97**, 6199 (1992).

[17] W. G. Lawrence and V. A. Apkarian, Isr. J. Chem. **30**, 135 (1990).

[18] M. W. Hill, R. Zadoyan, and V. A. Apkarian, Chem. Phys. Lett. **200**, 251 (1992).

[19] R. Zodoyan, and V. A. Apkarian, Chem. Phys. Lett. **206**, 475 (1993).

[20] R. D. Levine and B. Bernstein, *Molecular Reaction Dynamics and Chemical Reactivity* (Oxford University Press, Oxford, 1987).

[21] M. Polanyi, *Atomic Reactions* (Williams and Norgate, London, 1932).

[22] M. S. de Vries and R. M. Martin, Chem. Phys. **80**, 157 (1983); M. S. de Vries V. I. Srdanov, C. P. Hanrahan, and R. M. Martin J. Chem. Phys. **78**, 5582 (1983); M. S. de Vries, G. W. Tyndall and R. M. Martin, *ibid*. **81**, 2352 (1984); M. S. de Vries, G. W. Tyndall, C. L. Cobb, and R. M. Martin, *ibid*. **84**, 3753 (1986).

[23] (a) X. S. Chen and D. W. Setser, J. Phys. Chem. **95**, 8473 (1991); R. Sobczynski, D. W. Setser, and A. R. Slagle, J. Chem. Phys. **92**, 1132 (1990); (b) H. C. Brashears and D. W. Setser, J. Phys. Chem. **84**, 224 (1980); K. Tamagake, J. H. Kolts, and D. W. Setser, J. Chem. Phys. **71**, 1264 (1979).

[24] M. MacDonald, J. P. T. Wilkinson, C. Fotakis, M. Martin, and R. J. Dononvan, Chem. Phys. Lett. **99**, 250 (1983); B. V. O'Grady and R. J. Dononvan, *ibid*. **122**, 503 (1985); R. J. Donovan, P. Greenhill, M. A. Macdonald, A. J. Yencha, W. S. Hartree, K. Johnson, C. Jouvet, A. Kvaran, and J. P. Simon, Faraday Discuss. Chem. Soc. **84**, 221 (1987); R. J. Donovan, A. J. Holmes, P. R. R. Langridge-Smith, and T. Ridley, J. Chem. Soc. Faraday Trans. **85**, 541 (1988); J. P. T. Wilkinson, E. A. Kerr, K. P. Lawley, R. J. Donovan, D. Shaw, A. Hopkirk, and I. Munro, Chem. Phys. Lett. **130**, 213 (1986).

[25] E. D. Potter, J. L. Herek, S. Pedersen, Q. Liu, and A. H. Zewail, Nature **355**, 66 (1992).

[26] A. W. McCown and J. G. Eden, J. Chem. Phys. **81**, 2933 (1984).

[27] E. B. Gordon, V. G. Egorov, S. E. Nalivaiko, V. S. Pavlenko *et al.*, Chem. Phys. Lett. **242**, 75 (1995).

[28] W. G. Lawrence, K. C. Klemitshaw, and V. A. Apkarian, J. Geophys. Rev.-Atm. **95**, 591 (1990)

[29] C. R. Bieler, K. E. Spence, and K. C. Janda, J. Phys. Chem. **95**, 5058 (1991); C. R. Bieler and K. C. Janda, J. Am Chem. Soc. **112**, 2033 (1990).

[30] D. M. Proserpio, R. Hoffmann, and K. C. Janda, J. Am. Chem. Soc. **113**, 7184 (1991).

[31] S. D. Peyerimhoff and R. J. Buenker, Chem. Phys. **57**, 279 (1981); J. A. Coxon, *Molecular Spectroscopy* (The Chemical Society, London, 1973), Vol. 1.

[32] V. E. Bondybey and C. Fletcher, J. Chem. Phys. **64**, 3615 (1976).

[33] P. Gutler, H. Kunz, and J. Le Calve, J. Chem. Phys. **91**, 6020 (1989).

[34] J. G. McCaffrey, H. Kunz, and N. Schwentner, Chem. Phys. **96**, 155 (1992); H. Kunz, J. G. McCaffrey, R. Schriever, and N. Schwentner, *ibid*. **94**, 1039 (1991).

[35] R. L. Fulton, J. Chem. Phys. **61**, 4141 (1974).

[36] E. Quinones, Y. C. Yu, D. W. Setser, and G. Lo, J. Chem. Phys. **93**, 333 (1990).

[37] M. W. Hill, Ph.D. thesis, University of California, Irvine, 1995.

[38] M. Macler, J.-P. Nicolai, and M. Heaven, J. Chem. Phys. **91**, 674 (1989).

[39] J. Tellinghuisen and D. K. Chakraborty, Chem. Phys. Lett. **134**, 565 (1987); J. C. D. Brand and A. R. Hoy, Appl. Spectrosc. Rev. **23**, 285 (1987).

[40] M. Macler and M. Heaven, Chem. Phys. **151**, 219 (1991).

[41] I. Last and T. F. George, Chem. Phys. Lett. **183**, 547 (1991); J. Chem. Phys. **86**, 3787 (1987); **87**, 1183 (1987); I. Last, T. F. George, M. E. Fajardo, and V. A. Apkarian, *ibid.* **87**, 5917 (1987).

[42] E. C. Chen and W. E. Wentworth, J. Phys. Chem. **89**, 4099 (1985).

[43] M. E. Fajardo, V. A. Apkarian, A. Moustakas, H. Kreuger, and E. Weitz, J. Phys. Chem. **92**, 357 (1988).

[44] C. H. Becker, J. J. Valentini, P. Casavecchia, S. J. Sibener, and Y. T. Lee, Chem. Phys. Lett. **61**, 1 (1979).

[45] K, Balasubramanian, P. Feng, J. J. Kaufman, P. C. Hariharan, and W. S. Koski, Phys. Rev. A **37**, 3204 (1988).

[46] J. Le Clave and P. Gurtler, J. Chem. Phys. (Paris) **86**, 1849 (1989).

[47] H. Kunttu, E. Sekreta, and V. A. Apkarian, J. Chem. Phys. **94**, 7819 (1991).

[48] P. J. Hay and T. H. Dunning, J. Chem. Phys. **69**, 2209 (1978).

[49] See, for example, the treatment by F. Yu. Naumkin and P. J. Knowles, J. Chem. Phys. **103**, 3392 (1995).